J. Phys. Chem. 1992, 96, 5465-5472

thanks Prof. Mats Almgren for useful discussions.

Registry No. CTAC, 112-02-7; CTAB, 57-09-0; EHEC, 9004-58-4; Cl^-, 16887-00-6; pyrene, 129-00-0; cetylpyridinium chloride, 123-03-5.

References and Notes

(1) Goddard, E. D. *Colloids Surf.* **1986**, *19*, 255 and references therein.

(2) Saito, S. *Non-Ionic Surfactants-Physical Chemistry*; Schick, M. J., Ed.; Dekker: New York, 1989; Chapter 15 and references therein.

(3) Saito, S. *Kolloid Z.* **1957**, *154*, 19.

(4) Zana, R.; Lang, J.; Lianos, P. *Microdomains in Polymer Solutions*; Dubin, P., Ed.; Plenum Press: New York, 1985; p 357; *J. Phys. Chem.* **1985**, *89*, 41.

(5) Perron, G.; Francoeur, J.; Desnoyers, J.; Kwak, J. *Can. J. Chem.* **1987**, *65*, 990.

(6) Takahara, A.; Ichimaru, K.; Tashita, J. I.; Kumano, A.; Kajiyama, T.; Takayanagi, M. *Rep. Prog. Polym. Phys. Jpn.* **1983**, *26*, 669.

(7) Winnik, F.; Ringsdorf, H.; Venzmer, J. *Langmuir* **1991**, *7*, 905.

(8) Hoffmann, H.; Huber, G. *Colloids Surf.* **1989**, *40*, 181.

(9) Winnik, F.; Winnik, M.; Tazuke, S. *J. Phys. Chem.* **1987**, *91*, 594.

(10) Carlsson, A.; Karlström, G.; Lindman, B. *J. Phys. Chem.* **1989**, *93*, 3673.

(11) Carlsson, A.; Lindman, B.; Watanabe, T.; Shirahama, K. *Langmuir* **1989**, *5*, 1250.

(12) Carlsson, A.; Karlström, G.; Lindman, B. *Colloids Surf.* **1990**, *47*, 147.

(13) Karlström, G.; Carlsson, A.; Lindman, B. *J. Phys. Chem.* **1990**, *94*, 5005.

(14) Dualeh, A.; Steiner, C. *Macromolecules* **1991**, *24*, 112.

(15) Leung, P.; Goddard, E. D. *Langmuir* **1991**, *7*, 608.

(16) Malliaris, A.; Lang, J.; Zana, R. J. *J. Chem. Soc., Faraday Trans. 1* **1986**, *82*, 109.

(17) Zana, R. *J. Colloid Interface Sci.* **1980**, *78*, 330.

(18) Lindman, B.; Kamenka, N.; Kathopoulis, T. M.; Brun, B.; Nilsson, P. G. *J. Phys. Chem.* **1980**, *84*, 2485.

(19) Lindman, B.; Puyal, M. C.; Kamenka, N.; Rymdén, R.; Stilbs, P. *J. Phys. Chem.* **1984**, *88*, 5048.

(20) Gunnarsson, G.; Jönsson, B.; Wennerström, H. *J. Phys. Chem.* **1980**, *84*, 3114.

(21) From the variation of the cmc of dodecyltrimethylammonium chloride upon addition of NaCl,[22] we have obtained the following relationship for the change of the cmc of CTAC with the NaCl concentration, C_s: $\log \text{cmc} = -0.631 \log (\text{cmc} + C_s) - 6.286$. The 4.97 mM CTAC solution contained 1.07 mM (NaCl + $Na^{36}Cl$), which resulted in a cmc decrease of 25%. In the calculation of α from the diffusion data, the cmc values from the κ vs C plots were all reduced by 25%.

(22) Emerson, M.; Holtzer, A. *J. Phys. Chem.* **1967**, *71*, 1898.

(23) Zana, R.; Muto, Y.; Esumi, K.; Meguro, K. *J. Colloid Interface Sci.* **1988**, *123*, 502.

(24) Jada, A. Doctorate Thesis of the University Louis Pasteur, Strasbourg, **1988**.

(25) Zana, R. *Surfactants Solutions: New Methods of Investigation*; Zana, R, Ed.; Dekker: New York, 1987; Chapter 5.

(26) Nilsson, P.; Lindman, B. *J. Phys. Chem.* **1984**, *88*, 4764.

(27) Jönsson, B.; Wennerström, H.; Nilsson, P.; Linse, P. *Colloid Polym. Sci.* **1986**, *264*, 77 and references therein.

(28) Malliaris, A.; Le Moigne, J.; Sturm, J.; Zana, R. *J. Phys. Chem.* **1985**, *89*, 2708.

(29) Roelants, E.; Geladé, E.; Van Der Auweraer, M.; Croonen, Y.; De Schryver, F. C. *J. Colloid Interface Sci.* **1983**, *96*, 288.

(30) Roelants, E.; Geladé, E.; Smid, J.; De Schryver, F. C. *J. Colloid Interface Sci.* **1985**, *107*, 337.

(31) Roelants, E.; De Schryver, F. C. *Langmuir* **1987**, *3*, 209.

(32) Zana, R.; Yiv, S.; Strazielle, C.; Lianos, P. *J. Colloid Interface Sci.* **1981**, *80*, 208.

(33) Malliaris, A.; Binana-Limbelé, W.; Zana, R. *J. Colloid Interface Sci.* **1986**, *110*, 114.

(34) Lindman, B.; Carlsson, A.; Karlström, G.; Malmsten, M. *Adv. Colloid Interface Sci.* **1990**, *32*, 183.

(35) Karlström, G. *J. Phys. Chem.* **1985**, *89*, 4962.

(36) Zhang, K.; Karlström, G.; Lindman, B. *Prog. Colloid Polym. Sci.*, in press.

Oscillations in the Reaction Rate of Nitric Oxide Reduction by Ammonia over Polycrystalline Platinum Foil Catalysts

T. Katona[†,‡,§] **and G. A. Somorjai***[,†,‡]

Center for Advanced Materials, Materials and Chemical Sciences Division, Lawrence Berkeley Laboratory, 1 Cyclotron Road, Berkeley, California 94720, Department of Chemistry, University of California, Berkeley, California 94720, and Department of Organic Chemistry, Jozsef A. University, Dom ter 8., Szeged, H 6720 Hungary

(Received: November 12, 1991; In Final Form: February 7, 1992)

Self-sustained oscillations were obtained in the NO + NH_3 reaction at atmospheric pressure with reactant partial pressures of 133–600 Pa (1–4.5 Torr), in the temperature range of 603–673 K. The effects of reaction parameters, temperature, partial pressure, and reactant gas velocity were studied. The onset temperature of the oscillations (603 K) was slightly dependent on the partial pressure of nitric oxide in the feed gas. Near this temperature the oscillations were uncontrolled (chaotic), while increasing the temperature resulted in periodic oscillations in the reaction rates. The oscillation phenomena were studied in both isothermic and adiabatic modes. The oscillations, when initiated by a temperature increase, start up only after an induction period during which the rates of NO consumption and N_2 formation sharply increase as opposed to the slow enhancement of the rate of N_2O formation. The two reaction branches found at the high- and low-temperature regimes in the batch mode[1] have product distributions which are similar to those found at the extremes of the amplitudes of rate oscillations.

Introduction

Periodic oscillations in reaction rates, product concentrations or temperature have been observed in several heterogeneous catalytic reactions. This phenomena has attracted considerable attention as it is of both experimental and theoretical importance. Among these reactions were the oxidation of hydrogen,[2-5] carbon monoxide,[6-10] ethylene,[11] and ammonia.[12] Oscillations during reactions between nitric oxide and ammonia[13-15] as well as nitric oxide and carbon monoxide[16] have been observed over platinum catalysts. These experimental studies also generated a large number of modeling studies and theoretical developments.[17-23]

We have also studied the reduction of NO by ammonia using batch-mode measurements in the presence and absence of oxygen on polycrystalline foils of platinum of small surface area ($\simeq$2 cm^2).[1,25] We have also observed reaction oscillations in the absence of oxygen in the temperature range of 583–613 K and pressure range of 65–600 Pa (0.5–4.5 Torr) as the NO concentration was decreasing as a result of its reduction by ammonia.[1] To summarize our kinetic studies that we carried out over the platinum foil, we found a break on the Arrhenius plot in the temperature range of

---

[†] Lawrence Berkeley Laboratory.

[‡] University of California.

[§] Jozsef A. University.

0022-3654/92/2096-5465$03.00/0

573–603 K. The position of the break was dependent on the NO partial pressure; it was shifted toward higher temperatures with increasing NO pressures. In the lower temperature range (523–573 K), 102 kJ/mol activation energy was found, and the rate of nitric oxide consumption was zero order with respect to initial NO and NH_3 partial pressures. The rates of N_2 and N_2O formations gave a ratio of ≅1. In the high-temperature region of the reaction (573–613 K), the activation energy was 212 kJ/mol, and the consumption of the NO was first order with respect to NO initial partial pressure, and showed half-order dependence with respect to initial NH_3 partial pressure. In this temperature range the nitrogen product was dominant, giving an N_2/N_2O ratio above 10.[1]

We did not observe oscillations when molecular oxygen was present in the reaction mixture.[25]

The purpose of this paper is to focus on the oscillatory phenomena during the NO/NH_3 reaction over the platinum foil using mostly flow-mode experiments. We report how oscillations are ignited, maintained, and altered by changing the temperature, NO pressure, and flow rates. The effect of constant heating rate (adiabatic mode) is also studied.

Experimental Section

Apparatus. The reaction was carried out in an ultra-high vacuum (UHV) chamber which was equipped with a high-pressure cell. Using this system, the Pt foil samples were prepared and characterized by UHV surface science techniques and then isolated from the main chamber by the use of the high-pressure cell. It was connected to the gas manifold that allowed the use of batch-mode and flow-mode measurements as well. A detailed description of the manifold is given in ref 25. A base pressure of the main vacuum chamber was in the mid 10^{-8} Pa (10^{-10} Torr) range after 24-h bake out at 373 K. The background consisted of mostly CO, CO_2, H_2O, and air from the virtual leak of the sample manipulator.

The platinum foil (2.54×10^{-4} cm thickness, ≅2 cm^2 area) was spot welded to 0.5-mm-diameter gold wires welded to platinum pieces which were mounted on the copper rods of the manipulator. It was located in the middle of the chamber and allowed rotational movement, in order to align the sample to the Auger electron beam or the mass spectrometer.

A cross-sectional view of the reactor is given in Figure 1. The copper rods of the manipulator ended with platinum pieces in order to decrease thermal conductivity and keep the manipulator cold. We applied air flow through the hollow rods of the manipulator. The sample was resistively heated using precision temperature controllers. A chromel–alumel thermocouple was spot welded to the bottom middle edge of the platinum foil. Another thermocouple, immersed in an ice bath, was used as a reference.

Gases. NO (1%) in He, 1% NH_3 in He, 1% Ar in He, and 1% O_2 in He (Matheson certified standards) were used for the reaction without further purification. For the ion sputtering and oxygen annealing, high-purity Ar and O_2 were used, respectively. High-purity NO, NH_3, N_2, and N_2O (Matheson) were used for calibration. The isotope-labeled studies were carried out using 99% isotope purity ^{15}NO (Cambridge Isotopes).

Sample Preparation. The platinum foils were cleaned by subsequent ion sputtering (6.65×10^{-3} Pa (5×10^{-5} Torr) Ar, 2 kV, 30 mA, 15 μA) and O_2 annealing (973 K, 1.33×10^{-4} Pa, (10^{-6} Torr)). The surface was monitored by Auger electron spectroscopy (AES). Cleaning cycles were continued until the surface became free of contaminants as judged by AES. The only contaminant we found was carbon from the CO-, CO_2-containing environment of the UHV chamber. After the reaction in the batch mode, the AES spectra of the catalysts indicated the presence of N, O, and C. After several hours of work in the flow mode, we observed Cl (at 188 eV) on the surface in the extent of about 0.1 monolayer. This peak rapidly disappeared when the foil was heated up to 473 K.

Experimental Procedure. After cleaning the sample, the high-pressure cell was closed and the reactor was pressurized above atmospheric pressure with the 1% Ar in He internal standard. Then the exhaust valve of the reactor was opened and the gas flow through the reactor was set to the desired value. This way, back flow of the air of the outside environment was avoided.

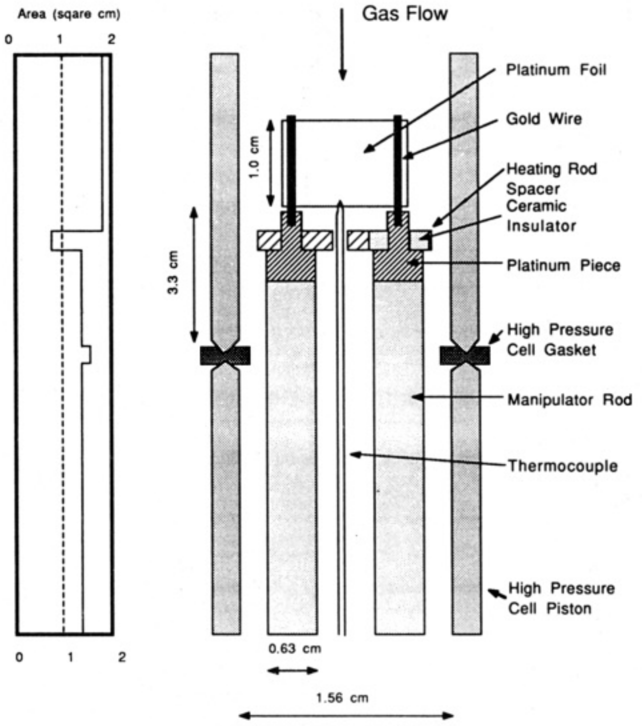

Figure 1. Schematic of the high-pressure cell with the platinum foil catalyst.

We utilized the leak of the high-pressure cell which occurred at the copper gasket 3.3 cm below the bottom edge of the catalyst to the UHV chamber. The closing hydraulic system of the high-pressure cell was adjusted to obtain 2.66×10^{-4} Pa (2×10^{-6} Torr) of pressure in the chamber, in order to get reactant partial pressures in the 10^{-6} Pa range. Since our reactants were in 1% concentration in He and all of the experiments were run at atmospheric pressure, the total pressure of non-helium compounds was always 1.03 kPa (7.6 Torr). We assumed that because of the high dilution of the gas mixture that leaked to the UHV chamber, the sensitivity of the ion gauge did not depend on the concentration. We used the Ar-containing He mixture for internal standard. By using the intensity at amu 40 and by assuming that it is proportional to the rate of the leak into the chamber, normalization of MS intensities as well as calibration were carried out for each compound. The calibrations for NO, Ar, N_2, and N_2O were verified by GC analysis.

The MS was connected to a programmable peak selector (PPS). We monitored 8 different channels at a rate of about 10–20/channel per minute. The PPS was on-line connected to an IBM-compatible PC via serial communication adapter. The data were stored in four-digit decimal ASCII numbers with a resolution of 0.01. Data files were evaluated using data handling software. The accuracy of N_2, NO, and N_2O measurements were within ±5%; however, during the oscillations when sudden changes in peak intensities occurred, the differences in pumping speed of the main vacuum system for these compounds became not negligible in contrast to the case of the batch reactor system with small changes in conversion.[1] In the case of NH_3 and H_2O, because of their strong adsorption capabilities and wall-pumping, the accuracy of the analysis was not better than ±10%.

In most of the cases, when isothermic reaction conditions were applied, a modified Eurotherm (7S 2162) precision temperature controller was used to set the temperature of the Pt foil. Because of the small volume of the catalyst and the direct heating current, the response time of the catalyst was very short; the temperature reached the preset value within ±1 K in less than 1 min. For the temperature-programmed reaction study, we used a Eurotherm 808 model precision temperature controller. The response time

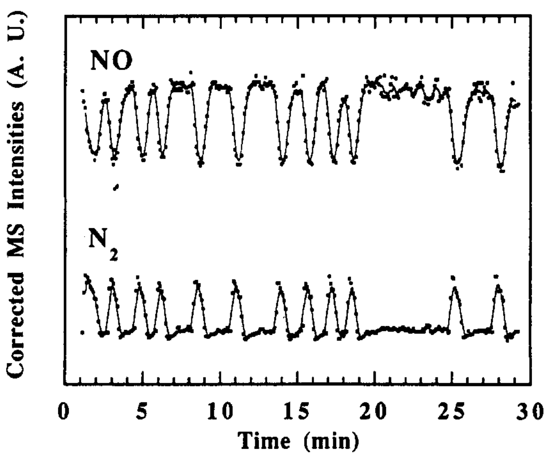

Figure 2. Uncontrolled (chaotic) oscillations obtained at 603 K at 150 cm^3/min flow rate. $P_{NO} = P_{NH_3} = 440$ Pa in the feed gas.

of this equipment was longer, thus especially in the region of oscillations, the accuracy of the temperature setting was ±2.5 K. For the adiabatic studies, an EMI TCR dc current supply connected to a 7S 3173 controller was used. For these studies, the thermocouple voltage was amplified with a signal conditioning amplifier (Measurements Group, type 2310) and connected to one of the analog inputs of the PPS. This way, synchronous recording of peak intensities and catalyst temperatures was carried out.

After setting flow rates using flow meters, the background pressure in the UHV chamber was set to 2.66×10^{-4} Pa (2×10^{-6} Torr). After 10 min, the catalyst was heated to the desired temperature, the PPS was started, and peak intensities were recorded taking into account of actual background intensities and multiple fragmentation patterns.

In Figure 1, the schematic of the reactor is shown. The reaction mixture after leaving the catalyst area are cooled to room temperature in contact with the air flow-cooled rods of the manipulator. The leak at the gasket of the high-pressure cell is utilized as a source of the MS analysis. It is likely that this leak mostly occurs at one point or certain location of the gasket because of the roughness of the knife-edge of the piston of the high-pressure cell, thus the leak is located to a particular point of the gasket. However, the gas stream in the reactor must be uniform since it does not depend on the rotational position of the manipulator. During the oscillations no effect can be seen when the manipulator is turned into any position. The intensity of the Ar internal standard is stable during the oscillations, showing that the gas flow in the reactor is uniform, no turbulencies occur, and the fluctuations in the reactant and product MS intensities are due to changes in their concentrations.[1]

The gas velocities for 100, 150, 200, 300, and 400 cm^3/min flow rates are 52.3, 78.5, 104.6, 157, and 209.2 cm/min in the catalyst area, respectively. Assuming a plug-like stream, the residence time of the gas in the catalyst area is in the range of 0.02–0.005 min, as compared to the cycle times of the oscillations in the range of 0.08–2.0 min. In fact, the cycle time of the oscillations was at least 1 order of magnitude higher than the residence time of the gases in the catalyst volume in each specific case we investigated.

Results

A: Procedure To Produce Oscillations during the NO + NH_3 Reaction by Increasing the Temperature at Constant Reactant Composition. The appearance of the oscillatory phenomenon is a function of temperature at a given NO concentration, i.e. increasing the temperature above a certain value, oscillations occur. Close to the lower temperature boundary of this regime, the cycle time is changing and the oscillations are uncontrolled (chaotic). In Figure 2, oscillations are shown, obtained at 603 K, which is close to this boundary, and the uncontrolled (chaotic) behavior is clearly seen. At 593 K, oscillations cannot be obtained using 440 Pa NO and 440 Pa NH_3 partial pressures in the feed mixture. In the 593–603 K range, depending on the temperature setting, using temperature controller with an accuracy of ±1 K, i.e. obtaining discrete changes in the temperature, nonperiodic, transient behavior can be observed. When the temperature is set to this range, a drop in the NO concentration occurs, indicating a jump in the consumption rate of nitric oxide, then the system is relaxed and a steady state is obtained. At higher temperatures (613 K and above), the oscillations are periodic with well-defined cycle times ($0 < \tau < 2.5$ min) which are functions of temperature and feed. Once started, it can be maintained for hours; the longest period of oscillations that we investigated was 240 min.

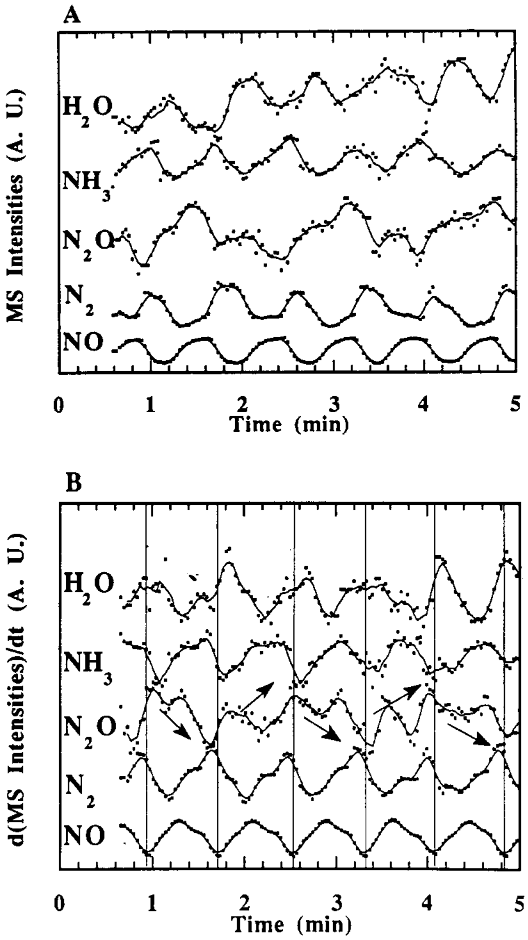

Figure 3. (A) Periodic changes in the product and reactant concentrations during "steady-state" oscillations (at 608 K; $P_{NO} = P_{NH_3} = 440$ Pa). The intensities are adjusted to the same scale for comparison. The increasing baseline of the H_2O curve is due to the increasing H_2O background. (B) Derivative curves of the concentration changes of Figure 3A. The periods, corresponding to the maxima in NO curve are also indicated.

The oscillations can be seen in the concentrations of all molecules leaving the catalytic reactor. These periodic changes are plotted in Figure 3A. The changes in the concentrations of reactants NO and NH_3 are in phase, and the changes in product concentrations N_2 and H_2O are concerted and in an opposite phase to the reactants. The rate of N_2O formation shows periodicity, too (double-peaked oscillations), but it is out of phase to the other molecules.[1] In Figure 3B, derivative curves of the concentration changes are shown. The changes in the rate of N_2O formation are periodic and exhibit periodicity with cycle time twice that of the single-peaked oscillations of the rate of NO consumption or N_2 formation. However, the derivative curve of the N_2O concentration exhibits a local minimum or inflexion in phase with the changes of the other molecules. The arrows show the tendencies of the changes in the curve; it is clearly seen that every second period is similar.

The temperature dependence of the oscillations is shown in Figure 4. By increasing the temperature (with 10 K units), the

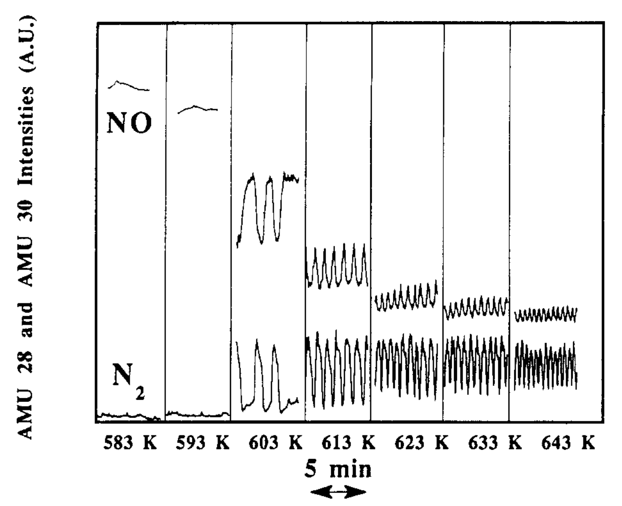

Figure 4. Steady states (583 and 593 K), uncontrolled oscillations (603 K), and periodic oscillations (613–643 K) at 150 cm^3/min flow rate and $P_{NO} = P_{NH_3} = 440$ Pa in the feed gas.

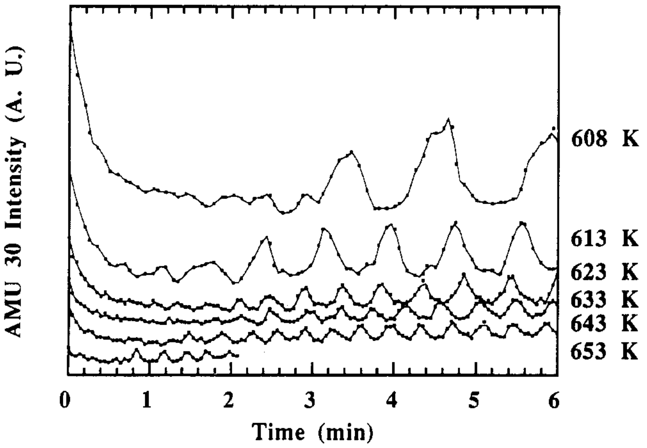

Figure 5. Induction periods at different temperatures. They are obtained by increasing the temperature 10 K. The new temperatures listed on the right-hand side of the graph are reached within 0.2 min. In the case of 608 K, the previous state of the system is unoscillatory, in all the other cases the system is forced from one oscillatory stage to another by this 10 K temperature increase.

frequency of the oscillations is increased while the amplitude is decreased. Above 653 K, the sampling rate of the PPS is not appropriate to follow the high frequency of the oscillations. By using analog sampling, it can be monitored in the 653–673 K range; above this temperature, the cycle time is decreased to below 1 s and the amplitude is declined to the level of the background noise.

B: Induction Period at the Onset of Oscillations of the NO + NH_3 Reaction. The oscillations described in section A are obtained using a fast-acting precision temperature controller, and the temperature is raised into the regime of the oscillations which is defined by both the NO partial pressure and the gas flow rate as well. Once inside this regime, oscillations occur; however, prior to the "steady-state" periodic oscillations, an induction period takes place. It is not necessary to cross the boundary of the oscillatory regime with the temperature to obtain the induction period. Even inside the oscillatory range, when the system is forced from one oscillating "steady state" to another by a relatively fast increase of the temperature, an induction period occurs prior to the new temperature-related oscillating conditions.

In Figure 5, for example, induction periods obtained by 10 K jumps of the temperature settings are plotted. The temperature reaches its new value within 0.2 min. Compared to this, a long induction period ($2.8_{608K} - 0.6_{653K}$ min) occurs, during which the NO conversion is high. Following this, oscillations appear with cycle times of $1.2_{608K} - 0.2_{653K}$ min. Note that the residence time of the gases in the catalyst area is 0.012 min (150 cm^3/min). The first few cycles of the oscillations have smaller amplitudes as compared to that of the "steady-state" oscillating system. In Figure 5, the zero on the time axis corresponds to the start points of the 10 K temperature jumps to the values indicated on the right-hand sides of the curves. Only in the case of 598–608 K temperature jump does the previous state of the system not shown oscillations.

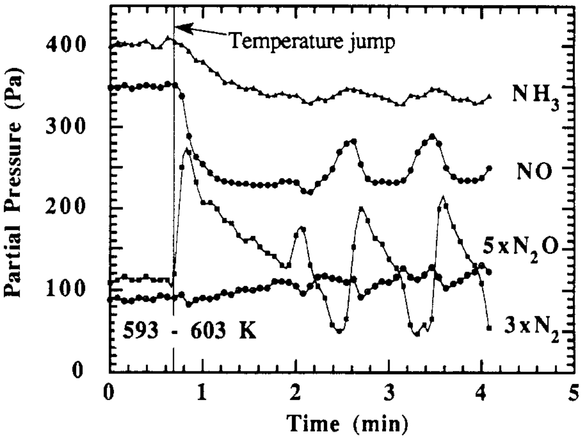

Figure 6. Reactants and product partial pressures before the temperature jump in steady state and after the temperature jump during the induction period and the oscillations. $P_{NO} = P_{NH_3} = 440$ Pa in the feed gas.

In Figure 6, the product distribution during the induction period is shown. When the temperature is increased, both the rate of NO consumption and the rate of N_2 formation jump suddenly. The rate of N_2O formation does not follow this—it is slowly increasing; while NO conversion is still high, it is taking over the N_2-producing branch of the reaction. At a certain N_2 and N_2O ratio, the rates of N_2 formation and NO conversion drop, and the cycle is started. However, the amplitude of the oscillation is increasing during a few cycles until the system reaches the "steady-state" amplitude. The higher the temperature, the more smaller cycles that take place prior to the "steady-state" oscillations.

C: Oscillations in the Temperature-Programmed Reaction Mode. During the steady flow of reactant gases over the platinum catalyst, the oscillations were started by increasing the temperature a certain amount. In this mode, a small increase in the temperature results in dramatic changes in the reaction rate and reaction pattern;[1] thus oscillations are started by a relatively strong influence on the system. However, the oscillations do occur when the temperature is increased slowly and gently using a temperature ramp controller. In Figure 7A, a temperature-programmed reaction is shown. The heating rate is 1 K/min. When it reaches the 603 K limit, oscillations are started and no induction period can be seen. The amplitude and cycle time are decreased with increasing temperature and are very close to those of the "steady-state" oscillations observed in the temperature-jump mode.

In Figure 7B, the same experiment is shown, but it is programmed from the higher temperatures down to the lower temperatures. As the temperature decreases the cycle time and amplitude increases and the average conversion is decreased. At the lower boundary of the oscillation range, the aperiodic relaxation-type oscillations are clearly seen. It is also seen that the shape of the two curves are different. Note that during the induction period the rate of NO consumption jumps to its highest value at that given temperature, i.e. the steeper slope of the heating-up curve can be due to the existence of the induction period, too, but the synchronization of the system resulting in oscillations is faster in this case.

D: Oscillations Using Constant Heating Power (Adiabatic Mode). In Figure 8A, oscillations are shown in the adiabatic mode. This way, a constant heating current is applied through the platinum foil. In the figure the temperature values are plotted as they were recorded synchronously with the MS intensities. However, they should be shifted right by about 0.03 min since the temperature of the catalyst is read immediately, while the gases

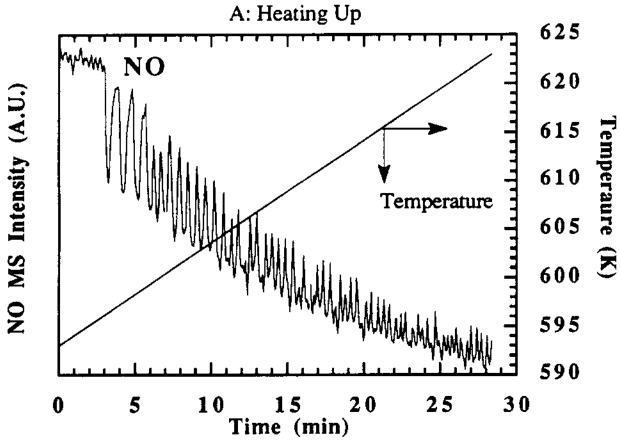

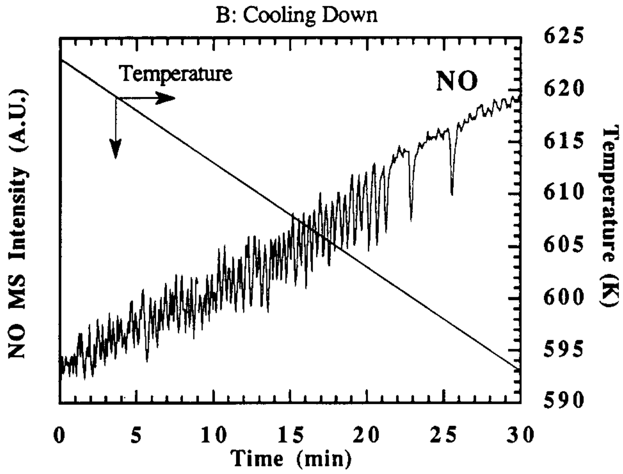

Figure 7. (A) Oscillations obtained by continuous temperature ramp, heating up. Flow rate is 150 cm^3/min $P_{NO} = P_{NH_3} = 440$ Pa in the feed gas. (B) Oscillations during continuous temperature ramp, cooling down period. Flow rate is 150 cm^3/min, $P_{NO} = P_{NH_3} = 440$ Pa in the feed gas.

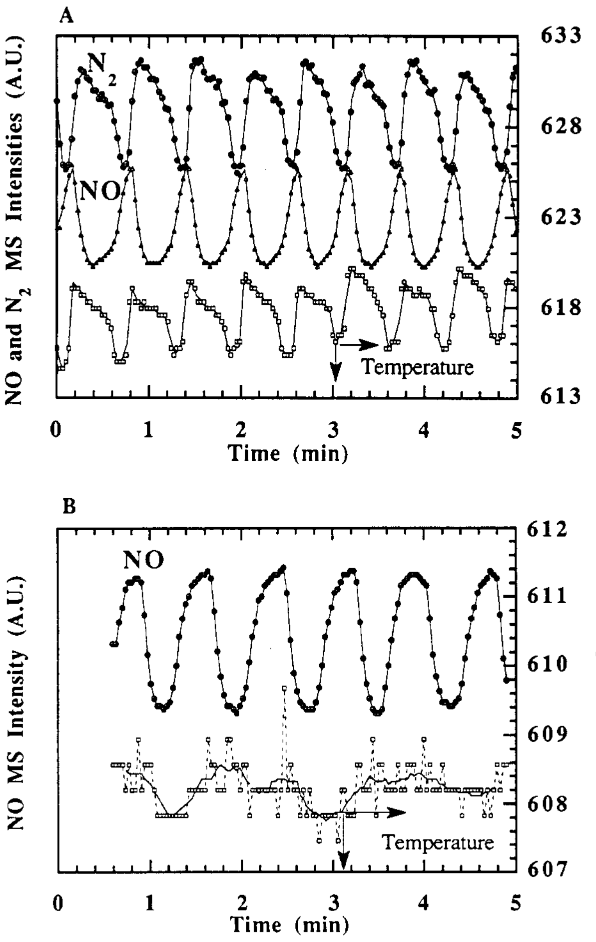

Figure 8. (A) Oscillations in adiabatic mode. The temperature changes are due the heat of the reaction and are in the range of 6 K. They are in phase of the oscillations. (B) Oscillations in isothermic mode when precision temperature controller is used. The temperature changes are in the range of ±0.5 K, and they do not show correlations with the oscillations.

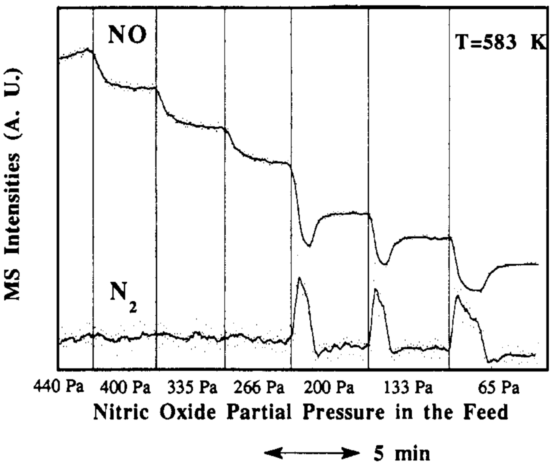

Figure 9. The effect of NO partial pressure on the stability of the system. At 583 K, using $P_{NO} = P_{NH_3} = 440$ Pa in the feed gas, no oscillations can be obtained. When the NO partial pressure is decreased below a certain value, transient behavior can be seen.

that leave the catalyst are sampled at the leak of the high-pressure cell gasket which is located 3.3 cm below the catalyst area. Note that the shape of the temperature curve and the N_2 concentration curve are almost identical. The changes in the catalyst temperature are due to the heat generated by the reaction and are in the range of 6 K.

For comparison, Figure 8B shows oscillations in an isothermic mode, when a precision temperature controller is used. The accuracy of controlling the temperature is ±0.5 K, and it does not show any correspondence with the oscillations.

E: Effect of NO Concentration on the Stability of the System and ^{15}NO-Labeled Studies in the Batch Mode. When the partial pressure of the NO is decreased at a given temperature just below the oscillatory range, transient behavior can be obtained. In Figure 9, results of an experiment are shown. The NO partial pressure is decreased while keeping the flow rate constant, partially replacing the NO-containing gas stream with He. When the partial pressure of NO is decreased below a certain level, the rate of NO conversion and N_2 formation jump and then they are relaxed, which resembles one cycle in the chaotic oscillation regime, but the phenomenon is not continued; this oscillation is aperiodic.

Instead of applying a certain pressure drop, the NO concentration can be decreased continuously by the reaction itself in the batch mode. During the reaction, NO is consumed, and when its partial pressure drops below a certain level, oscillations start and the transition between the two reaction patterns occurs.[1] This effect can be seen in Figure 10, where ^{15}NO is used in the reaction mixture. The initial NO partial pressure is 480 Pa, and the pressure of NH_3 is 400 Pa.[1] The temperature of the reaction is 583 K. When the ^{15}NO (amu 31) drops below about 220 Pa (also see Figure 9), oscillations occur. Note that in the high-pressure reaction regime the rates of the formation of nitrous oxide (N_2O) and nitrogen are about the same. It should be noted that in the high-pressure regime of the reaction the $^{15}N_2^+$ (amu 30) peak intensity is mostly due to the fragmentation of $^{15}NO_2O^+$ (amu 46) parent molecular ions. In the high-pressure regime, the lack of either $^{14}N^{15}NO$ (amu 45) or $^{14}N_2O$ (amu 44) indicates that no reaction leading to nitrous oxide occurs between ^{15}NO and $^{14}NH_3$ and the formation of $^{15}N_2O$ is due to two ^{15}NO molecules. However, the main nitrogen product is mixed $^{14}N^{15}N$, indicating that the nitrogen-producing path of the reaction involves both the

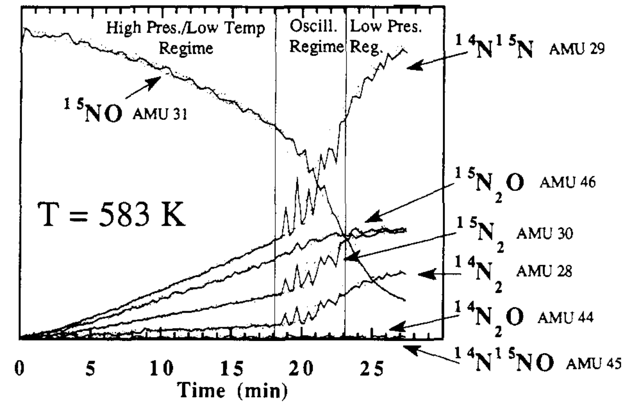

Figure 10. Oscillations obtained in the batch mode using ^{15}N-labeled nitric oxide. According to ref 1, the system exhibits the features of the high NO pressure regime and low NO pressure regime. Between them, in the transition range, oscillations occur. Note that in the high-pressure regime, the amu 30 signal is mainly due to the fragmentation of amu 46 ($^{15}N_2O$), while during the oscillations the change of the ratio of these intensities indicates that $^{15}N_2$ molecule is also produced. [Initial ^{15}NO pressure = 480 Pa; initial $^{14}NH_3$ pressure = 400 Pa.]

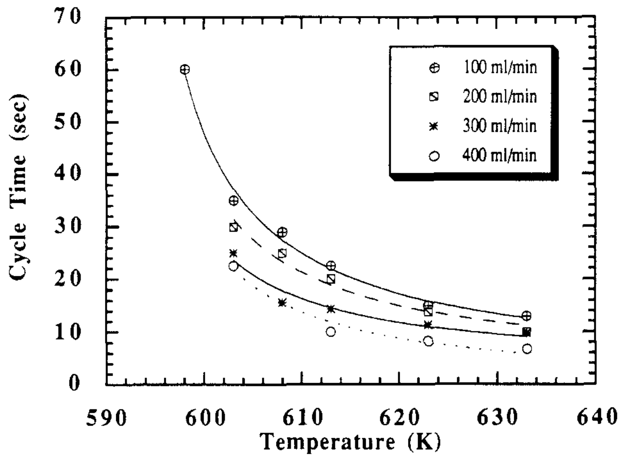

Figure 11. Cycle times of oscillations at different temperatures and flow rates; NO and NH_3 pressures in feed: 440 Pa.

NH_3 and NO molecules. Next to the dominant mixed nitrogen formation we found $^{14}N_2$ molecules, which were recombination products of NH_x surface species, while in the high-pressure range the $^{15}N_2$ (amu 30) intensity was mainly due to the fragmentation of $^{15}N_2O$ (amu 46) molecules in the mass spectrometer.

In the oscillation regime, the rate of NO consumption jumps, indicating that the activity of the catalyst is sharply increased. This results in a sudden jump in the $^{14}N^{15}N$ product; however, the $^{15}N_2O$ formation is suppressed while both $^{14}N_2$ and $^{15}N_2$ formations are enhanced, indicating that during this period the recombination probability of N atoms on the surface is higher.

In the low-pressure regime, the main product of the reaction is $^{14}N^{15}N$, while $^{15}N_2O$ formation is still slow, and the $^{14}N_2$ product shows that the recombination of $^{14}NH_x$ species exists as well. Its higher formation rate indicates that the probability of recombination is higher at these low nitric oxide partial pressures.

F: **Effect of the Change in Flow Rates on the Oscillations.** It has been shown that the cycle time of the oscillations is shorter at higher temperatures (Figures 4 and 7A,B). In Figure 11, cycle times of oscillations are shown at different temperatures and flow rates. Generally, at the same temperature, the higher the flow rate, the shorter the cycle time that is obtained.

In Figure 12, the frequencies of the oscillations are plotted vs the temperature of the catalyst. Linear correspondence is observed; the slope does not show dependence on the flow rates.

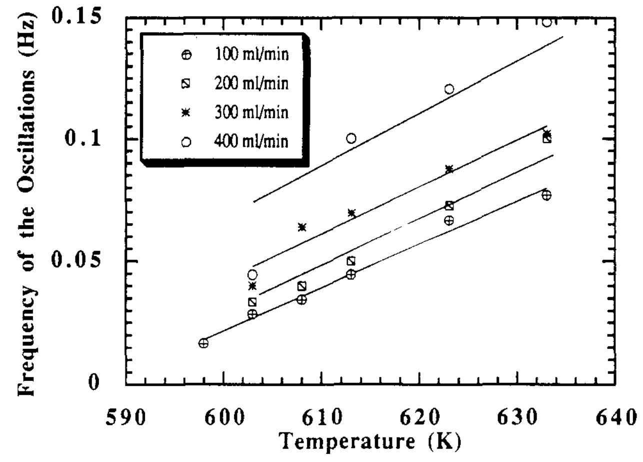

Figure 12. Frequencies of the oscillations as a function of temperature at various flow rates; NO and NH_3 pressures in feed: 440 Pa.

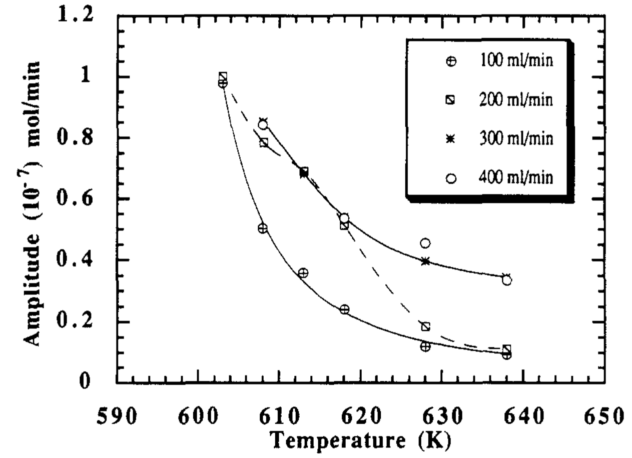

Figure 13. Amplitude of the oscillations as a function of temperature at various flow rates. At 603 K, all of the systems regardless of the flow rate exhibit the same amplitude. Above this temperature, as the overall reaction rate is increased, the amplitude of the oscillations at 100 mL/min flow rate becomes mass transfer limited. Above 618 K, the amplitude of the oscillations at 200 mL/min flow rate also becomes mass transfer limited.

If the amplitude is expressed in reaction rate units (Figure 13), the amplitude of the oscillations does not depend much on the flow rate at lower temperatures and the flow rates above 150 mL/min. At the lowest temperature (603 K) at which oscillations are obtained, the amplitude of the oscillations, i.e. the difference between the extremes of the rates of NO consumption in the system, is nearly the same regardless of the applied flow rate. When the temperature is raised and thus the overall reaction rate is increased, the 100 mL/min flow rate curve shows lower amplitude than the other flow rate curves, suggesting the existence of mass-transfer limitations. Above 618 K, the 200 mL/min flow rate curve also declines to the level of the 100 mL/min curve, showing that above this temperature the overall rate of NO consumption becomes higher than is necessary for the original kinetics and the reaction becomes mass transfer limited. However, if 300 mL/min or higher flow rates are applied, the amplitude of the oscillations does not depend on the flow rate, i.e. in this regime the oscillatory phenomena are not driven or controlled by mass transfer limiting conditions.

However, it should be mentioned that even at lower temperatures and higher flow rates the cycle time does not depend on the flow rate, indicating the importance of reactor geometry and total mass flow, just like in refs 13–15.

Discussion

Platinum seems to be an excellent catalyst for studies of oscillatory reactions. For example, oscillations in the CO oxidation reaction were observed on Pt(100),[26,27] polycrystalline Pt foil,[28-30] and supported platinum.[17,18,31] The reaction between NO and CO was accompanied with oscillations on Pt(100).[16]

Several models have been proposed to account for the periodic variations of the reaction rates. These include periodic oxidation and reduction of some parts of the metal surface, surface reconstruction, adsorbate–adsorbate interactions, and multiple steady states of the same reactions.

To our knowledge, this is the second observation of oscillations in the nitric oxide and ammonia reaction. Schmidt and co-workers, using polycrystalline platinum wires in the 0.1–1 Torr total pressure range, obtained oscillations in the 673–783 K temperature range.[14] Their reactor was a stirred tank type, and the total pressure was set by changing the differential pumping speed. Because of the low pressure and relatively low conversions, boundary layer effects and mass-transfer limitations did not play role. Modeling of the system[15] based on the proposed mechanism,[14] which was capable of describing product distributions in a very wide range of concentration and temperature parameters, indicated the importance of the reactor geometry and mass flow of the limiting compound on the oscillatory behaviors of the catalytic reaction.[15] In our system, because of the atmospheric pressure we used, boundary layer effects are not negligible. In some cases, the conversion is as high as 70%; thus mass transfer limitations could exist. The use of helium as an inert gas carrier results in high thermal conductivity of the gases, which can be easily seen in the adiabatic experiment where the amplitude of the temperature changes does not exceed 6 K (Figure 8A). Keeping in mind these differences, however, several similarities between our results and Schmidt's results should be emphasized, such as the close temperature ranges, the reaction rates (TOFs $\cong 10\ s^{-1}$), and the temperature dependence of the cycle time of oscillations. It should be mentioned that the N_2O formation is out of phase with respect to the formation or consumption of other components in both systems. Because of these similarities we use their suggested mechanism published in ref 13 in our discussion as well.

Additionally, there are differences we found in our system. When the catalyst is heated to the desired temperature, using a fast-acting precision temperature controller, an induction period precedes the oscillatory stage, and except for N_2O formation single-peaked oscillations occur in both the isothermic and adiabatic reaction mode. Because of the high thermal conductivity of our gas mixture, the adiabatic reaction conditions do not differ seriously from the isothermic conditions.

In our case, the oscillatory phenomena can be qualitatively described using our kinetic observations about the system[1] in accordance with the mechanism published in ref 13. According to the batch-mode experiments,[1] the Arrhenius plot of the reaction exhibits a break in the 573–603 K regime. Obviously, the two 212 and 102 kJ/mol activation energy slope portions of the curve represent different reaction patterns. One is the high NO partial pressure/low temperature reaction path where considerable N_2O formation takes place. The N_2O molecule is derived from two NO molecules (Figure 10). This is in agreement with Otto and Shelef's results,[32] as they found that the N_2O formation was dominantly from two NO molecules. The somewhat lower selectivity that they obtained could be due to the remarkably higher partial pressures and supported Pt they used.

In the high-temperature/low NO partial pressure region the N_2 formation is dominant, and the N_2 molecules are produced mostly from the NO and NH_3 molecules.[1]

The extremes of the oscillations can be related to these two reaction patterns. The overall stoichiometries of the NO + NH_3 reaction leading to N_2 and N_2O are

$$6NO + 4NH_3 = 5N_2 + 6H_2O\ (\Delta H^\circ_{298} = 295\ kJ/mol) \quad (1)$$

$$8NO + 2NH_3 = 5N_2O + 3H_2O\ (\Delta H^\circ_{298} = 112\ kJ/mol) \quad (2)$$

The temperature changes in the adiabatic mode indicate that when the rate of N_2 formation is the highest the temperature of the catalyst is also increased, showing that the more exothermic reaction (eq 1) is dominant. However, when the rate of N_2 formation is the lowest, especially in the isothermic mode,[1] the rate of N_2O formation is high compared to its lowest formation rate and makes a greater contribution to the removal of NO. This effect can also be seen on Figure 3, parts A and B, where N_2O oscillations are double peaked, but the lowest concentration values always correspond to the peaks in N_2 formation.

According to refs 13 and 14 the mechanism of the reaction is

$$NH_3 + 2S \rightleftharpoons NH_2\text{-}S + H\text{-}S \quad (3)$$

$$NO + S \rightleftharpoons NO\text{-}S \quad (4)$$

$$NH_2\text{-}S + NO\text{-}S \rightleftharpoons N_2 + 2S + H_2O \quad (5)$$

$$H\text{-}S + NO\text{-}S \rightarrow HNO\text{-}S + S \quad (6)$$

$$2HNO\text{-}S \rightarrow N_2O + H_2O + 2S \quad (7)$$

$$HNO\text{-}S + H\text{-}S \rightarrow N\text{-}S + H_2O + S \quad (8)$$

$$2N\text{-}S \rightarrow N_2 + 2S \quad (9)$$

Equations 5 and 7 represent the major reaction paths. Our previous findings in the batch mode[1] are in agreement with this. As is indicated in Figure 10, the N_2O formation is completely due to two NO-originated surface species (eq 7). Thus a reaction (eq 10) leading to N_2O from NO and NH_3 can be excluded.

$$NH_2\text{-}S + NO\text{-}S \rightarrow N_2O + 2H\text{-}S \quad (10)$$

Also, this mechanism explains the differences between the product distributions found in the high-pressure range and the low-pressure regime. When NO is in high concentration (high-pressure regime), the concentration of HNO–S species is higher, thus more N_2O is forming (eq 7). In the low-pressure regime the N_2 formation is dominant (eq 5). However, during the oscillations a reaction path that gives rise to N_2 formation from two NH_3-originated surface species also exists. The fact that at high NO concentrations step 5 is relatively suppressed might indicate that NO and NH_3 adsorb competitively.

As it has been pointed out by Takoudis and Schmidt,[13] the above mechanism itself can describe steady-state reaction rates and product distributions in a very wide range of parameters. For example, it can explain the lack of N_2O formation in UHV[33] at low NO coverages, the temperature-independent N_2O:N_2 ratio at high (60 Torr) NO pressures,[32,34] and the temperature-dependent N_2O:N_2 ratio at intermediate (0.1–3 Torr) NO pressures as well. It also gives a good estimate of the reaction rate over this wide pressure and temperature range.[13] Takoudis and Schmidt[13] reported oscillations in a well-stirred steady-state tank reactor with conversions of 1–5%; thus pure kinetic reasons first accounted for the oscillations, and all bulk phase mass balances were neglected. This treatment did not result in oscillations.[15] When the reactor mass balance was also included into the differential equation system, the model led to prediction of oscillatory states. The simulated transient oscillations exhibited N_2O formation out-of-phase to the other molecules,[15] which is in agreement with our observations; thus we believe that the mechanism presented in ref 13 is valid in our case as well.

These results indicate that single-peaked oscillations can be mathematically obtained with at least two autonomous equations; however, in the case of heterogeneous catalytic reactions, bulk-phase mass balances should be taken into account since they may drastically alter the dynamics of the system.[15]

However, the existence of the induction period indicates that when the temperature is increased, the N_2 formation jumps immediately along with the NO consumption rate. It means that at the beginning of this process there is no molecule adsorbed on the surface which inhibits the reaction that leads to N_2 formation. In other words, the surface is most active for the N_2 formation. The appearance of $^{14}N_2$ and $^{15}N_2$ (Figure 11) during the oscillations indicates that chemisorbed N atoms derived from both NH_3 and NO exist on the surface.

During the induction period, the rate of N_2O formation slowly increases and N_2 formation decreases, which indicates that the probability of the reaction of two NO molecules (or NO-related surface species) increases, since we saw that the only source of N_2O formation is a reaction between two NO-originated species both in the high-pressure regime and oscillation range as well. During the induction period, as the rate of the N_2O formation increases, the reaction between NO and NH_3 related surface complexes to produce N_2 is gradually inhibited, and at one point, this inhibition results in the complete drop in the N_2 formation path of the reaction (Figure 6). This could be due to the inhibition of NH_3 dissociation or adsorption, since NO conversion is still high. The existence of an induction period may indicate that synchronization also occurs prior to the oscillations; thus the ignition of the oscillation can be a surface reconstruction or a phase transition between oxidized and reduced domains of the metal surface. These processes may occur in the same period as the oscillations, thereby driving the reaction rate fluctuations.

The transition between the two reaction paths can be obtained by decreasing the NO partial pressure at lower temperatures as well. In Figure 10, it is clearly seen that while working in the high-pressure region, the formation of the N_2 does not depend on the NO partial pressure, i.e. it is zero order with respect to NO partial pressure. When the system is in the low-pressure region, the rate of N_2 formation depends on the NO partial pressure. The linear dependence of the frequency of the oscillations on the temperature might indicate that an adsorbate-related/induced surface phase transition is the driving force of the oscillation (Figure 12).

Surface science studies of NO and NH_3 desorption at different coverages have been carried out.[35] NO desorbs in the 400–600 K range, and NH_3 desorbs at lower temperatures than NO. NO and NH_3 can be readily coadsorbed at 150 K as long as NO is adsorbed first. The preadsorption of NH_3 blocks NO adsorption. It should be noted that the NO desorption temperature is close to the onset of oscillations in the NO/NH_3 reaction. However, dissociation of NO also occurs in the extent of about 20% of the saturation coverage. The highest rate of N_2 desorption is at 500 K, but the O_2 leaves the surface only above 673 K. Coadsorbed oxygen suppresses N_2 formation, but N_2O formation remains possible. This coadsorbed oxygen can react with hydrogen from ammonia dissociation[36] and may provide oxide and metal phases on the surface supplying the driving force of the oscillations by their periodic collapse/growth. The induction period certainly suggests that synchronization plays a role during oscillations.

The dependence of oscillations on the reactor geometry is complex. When the platinum foil is rotated in the reaction chamber, there is no effect on the oscillation behavior; thus we believe that the reactor geometry itself is not responsible for the effect we observe. However, the gas velocity, i.e. the transport of the reacting compounds, influences the cycle time of the oscillations, indicating the importance of these parameters as it has been pointed out by the literature.

Summary

Sustained oscillations were obtained in the catalytic reduction of nitric oxide by ammonia over polycrystalline platinum foils with partial pressure of the reactants in the range of 133–600 (1–4.5 Torr) in He. The oscillations occurred when the temperature was set in the oscillatory range, either by increasing it with discrete values or with continuous ramping. The onset temperature was well defined by the nitric oxide partial pressure in the feed and gas flow rate through the reactor. Near to this temperature, the oscillations exhibited the longest cycle times and were uncontrolled (chaotic). When using discrete temperature increases ($\Delta T/\Delta t > 10$ K/min), an induction period preceded the periodic oscillations. The cycle times of the periodic oscillations were in the range of 1.2–0.017 min; above 673 K, the amplitude and cycle time decreased below the experimental detection limits.

The extremes of the oscillations can be qualitatively described based on the batch-mode observations of the system.[1] Two reaction paths with different activation energies and product distributions corresponding to the high NO pressure and low NO pressure regimes were found. Between them a transition range occurred which was accompanied by rate oscillations. In the flow mode, just below the onset temperature of the oscillations at given feed concentrations, the system exhibited transient behavior (aperiodic, relaxation-type oscillation), similar to that observed in the uncontrolled oscillations regime.

The cycle time of the oscillations decreased with increasing flow rate of the reactant gas mixture; the observed frequency exhibited a linear correlation with the temperature with a slope independent of the flow rate. The amplitude of the oscillations was not dependent on the flow rate at lower temperatures (603–653 K) and flow rates higher than 150 cm^3/min, indicating that no mass transfer limitations occurred under those conditions.

However, the influence of the gas velocity on the oscillation parameters emphasizes the complexity of the whole reactor system, and the need of complex modeling studies, which are planned as a future work in our laboratory.

Acknowledgment. This work was supported by the Director, Office of Energy Research, Office of Basic Energy Sciences, Materials Science Division, U.S. Department of Energy, under Contract No. DE-AC03-76SF0098.

Registry No. NO, 10102-43-9; ammonia, 7664-41-7; platinum, 7440-06-4.

References and Notes

(1) Katona, T.; Guczi, L.; Somorjai, G. A. *J. Catal.*, in press.

(2) Belyaev, V. D.; Slinko, M. M.; Slinko, M. G.; Timoshenko, V. I. *Kinet. Katal.* **1973**, *14*, 810.

(3) Belyaev, V. D.; Slinko, M. M.; Slinko, M. G.; Timoshenko, V. I. *Dokl. Nauk. SSSR.* **1974**, *214*, 1098.

(4) Belyaev, V. D.; Slinko, M. M.; Timoshenko, V. I. *Kinet. Katal.* **1975**, *16*, 555.

(5) Beuch, H.; Fieught, P.; Wicke, E. *Chem. Ind. Tech.* **1972**, *44*, 445.

(6) Dawies, W. *Philos. Mag.* **1934**, *17*, 233.

(7) Dawies, W. *Philos. Mag.* **1935**, *19*, 309.

(8) Hugo, P.; Jakubith, M. *Chem. Ing. Technol.* **1972**, *44*, 383.

(9) Cardoso, M. A. A.; Luss, D. *Chem. Eng. Sci.* **1969**, *24*, 1699.

(10) Dauchot, J. P.; Cakenberghe, J. v. *Nature (London)* **1973**, *249*, 61.

(11) Schwartz, A.; Holbook, L. L.; Wise, H. *J. Catal.* **1971**, *21*, 199.

(12) Stephanopoluos, M. F.; Schmidt, L. D.; Caretta, R. *J. Catal.* **1980**, *64*, 301.

(13) Takoudis, C. G.; Schmidt, L. D. *J. Phys. Chem.* **1983**, *87*, 958.

(14) Takoudis, C. G.; Schmidt, L. D. *J. Phys. Chem.* **1983**, *87*, 964.

(15) Nowobilski, P.; Takoudis, C. G. *Chem. Eng. Commun.* **1985**, *33*, 211.

(16) Schwartz, S. B.; Schmidt, L. D. *Surf. Sci.* **1986**, *206* (1–2), 169.

(17) Sheintuch, M.; Schmitz, R. A. *Catal. Rev. Sci. Eng.* **1977**, *15*. 107.

(18) Slinko, M. G.; Slinko, M. M. *Catal. Rev. Sci. Eng.* **1978**, *17*, 119.

(19) Eigenberger, G. *Chem. Eng. Sci.* **1978**, *33*, 1263.

(20) Schuth, F.; Song, X.; Schmidt, L. D.; Wicke, E. *J. Chem. Phys.* **1990**, *92* (1), 745.

(21) Constantine, A. P.; Luss, D. *Chem. Eng. Sci.* **1977**, *32*, 191.

(22) Eiswirth, R. M.; Krisher, K.; Ertl, G. *Appl. Phys. A* **1990**, *A51* (2), 79.

(23) Kordesh, M. E.; Engel, W.; Lapeyre, G. J.; Zeitler, E.; Bradshaw, A. M. *Appl. Phys. A* **1989**, *A49* (4), 399.

(24) Reference deleted in press.

(25) Katona, T.; Guczi, L.; Somorjai, G. A. *J. Catal.*, in press.

(26) Ertl, G.; Norton, P. R.; Rustig, J. *Phys. Rev. Lett.* **1982**, *49*, 177.

(27) Cox, M. P.; Ertl, G.; Imbihl, R.; Rustig, J. *Surf. Sci.* **1983**, *134*, L517.

(28) Burrows, V. A.; Sundaresan, S.; Chabal, Y. J.; Christman, S. B. *Surf. Sci.* **1985**, *160*, 122.

(29) Yeates, R. C.; Turner, J. E.; Gellmann, A. G.; Somorjai, G. A. *Surf. Sci.* **1985**, *149*, 175.

(30) Turner, J. E.; Sales, B. C.; Maple, M. B. *Surf. Sci.* **1981**, *103*, 54.

(31) Kaul, D. J.; Wolf, E. E. *J. Catal.* **1985**, *91*, 216.

(32) Otto, K.; Shelef, M.; Kummer, J. T. *J. Phys. Chem.* **1970**, *74*, 2690.

(33) Gland, J. L.; Korchak, V. N. *J. Catal.* **1974**, *33*, 376.

(34) Pusateri, R. J.; Katzer, J. R.; Manogue, W. H. *AIChE J.* **1974**, *20*, 219.

(35) Katona, T.; Somorjai, G. A. Submitted to *Langmuir*.

(36) Katona, T.; Plummer, C.; Morand, A. J.; Somorjai, G. A. Submitted to *Appl. Catal.*